ELSEVIER

Journal of Luminescence 86 (2000) 399–405

JOURNAL OF LUMINESCENCE

www.elsevier.com/locate/jlumin

Spectral hole burning in naphthalocyanines derivatives in the region 800 nm for holographic storage applications

A.V. Turukhin[a,1], A.A. Gorokhovsky[a,*], C. Moser[b], I.V. Solomatin[b], D. Psaltis[b]

[a]*The College of Staten Island and Graduate School of CUNY, 2800 Victory Blvd., Staten Island, NY 10314, USA*
[b]*California Institute of Technology, Pasadena, CA 91125, USA*

Abstract

Persistent spectral hole burning is studied for several free-based and metallo-naphthalocyanine derivatives in polymer hosts. These materials exhibit a strong 0–0 absorption band in the region 800 nm matching the wavelength range of most semiconductor diode lasers and Ti : Sapphire lasers. Metallo-naphthalocyanines demonstrate a nonphotochemical hole-burning mechanism that is likely related to rotations of small molecular groups attached to a relatively rigid molecular ring. Free-base molecules exhibit the regular proton phototautomerisation mechanism of hole burning. Spectral- and hole-burning parameters were determined for eight materials; in particular, the hole-burning kinetics was analyzed and the quantum efficiencies were determined to be between 0.1% and 1%. Holograms (data pages) in the transmission geometry were successfully recorded in the materials studied using single-frequency laser diodes.

Keywords: Hole burning; Naphthalocyanines; Holography

1. Introduction

Porphyrin and phthalocyanine derivatives in polymer hosts have been extensively studied as potential materials for frequency- and time-domain spectral hole-burning optical storage. These materials exhibit S_0–S_1 0–0 absorption bands in the red wavelength region (610–700 nm), large inhomogeneous broadening and relatively narrow holes at low temperatures, and a built-in proton phototransformation mechanism between different tautomers in free-base compounds. More complex options to porphyrins and phthalocyanines are naphthalocyanines. Due to the increase in size of their skeleton and π-electron system, these molecules have 0–0 absorption patterns shifted towards the infrared. A persistent spectral hole burning (PSHB)-based memory has the potential of ultra-high storage density (Tbyte/cm^2) in polymer-based materials. Recently, the recording of 12,000 holograms in one spatial location using frequency multiplexing around 634 nm has been demonstrated in chlorine-doped polyvinyl butyral films [1]. To access holograms stored in the medium, the laser source is tuned to the corresponding wavelength used to record the hologram. The laser frequency tunability has to match the

* Corresponding author. Tel.: +1-718-982-2815; fax: +1-718-982-2830.

E-mail address: gorokhovsky@postbox.csi.cuny.edu (A.A. Gorokhovsky)

[1] Present address: Research Laboratory of Electronics, MIT, Cambridge, MA 02139, USA.

0022-2313/00/$ - see front matter
PII: S0022-2313(00)00182-4

inhomogeneous linewidth of the material, which is typically 10 THz for polymer-based materials. The accuracy and repeatability of the laser source must be less than the homogeneous linewidth; for polymers at 4.2 K it is less than or about 1 GHz. Fast tuning between frequency channels is required for fast data transfer. In the infrared region, laser sources such as distributed feedback lasers are commercially available. These laser diodes are excellent sources for polymers sensitive in the IR, because they provide good stability and repeatability ($\ll$1 GHz), fast tunability (5 ns for current tuning), and a relatively large scanning range ($\sim$3 nm).

We report here on an investigation of the spectral- and hole-burning properties of five commercially available free-based and metallo-naphthalocyanines in two polymer hosts and their application for high-fidelity holography. These materials exhibit a strong 0–0 absorption band in the 800 nm region.

2. Samples

The samples under investigation were five naphthalocyanines derivatives: 2,11,20,29-tetra-tert-butyl-2,3-naphthalocyanine (H_2-TBNP), 1,4,8,11, 15,18,22,25- octabutoxy-2,3-naphthalocyanine (H_2-OBNP), zinc 2,11,20,29-tetra-tert-butyl-2,3-naphthalocyanine (Zn-TBNP), nickel 2,11,20,29-tetra-tert-butyl-2,3-naphthalocyanine (Ni-TBNP), and silicon 2,3- naphthalocyanine dioctyloxide (Si-NPDO). To prepare the samples we used two types of host matrix: polyvinyl butyral (PVB) for samples with thickness in the range of 100–400 μm, and polystyrene (PS) to produce samples with thickness larger than 1 mm. The doping concentration was between 10^{-3} and 10^{-5} mol/l.

Samples with good optical quality where prepared as follows. The dopants where purchased in powder form from Aldrich and without further purification diluted in acetone. After evaporation, the PVB powder was mixed with the diluted dopant in dichloromethane. The mixture was left for evaporation for 2 days in a Petri dish. The resulting thin films where then pressed against a polished metal plate at 75°C to achieve good optical quality.

To prepare polystyrene samples, the dopant powder was mixed with purified styrene in a pyrex container. The containers was then cooled in liquid nitrogen and vacuum pumped to remove the oxygen. The container is then heated in hot water. The cycle is repeated 4 times. The pyrex container is then sealed and left at 100°C for 2 days for polymerization.

3. Spectral- and hole-burning properties

Absorption spectra of the several representative materials at 8 K in the region of the S_1–S_0 transition are shown in Fig. 1. All materials studied have the intense 0–0 band located around 790 nm. Some impurities, particularly H_2-TBNP, display strong signs of aggregation at concentration higher than 10^{-4} mol/l as it can be seen by comparing Figs. 1(a) and (b).

Spectral holes were burned in the 0–0 absorption band and detected in transmission by a single-frequency tunable Ti : Sapphire laser with linewidth less than 1 MHz at the temperature 1.5 K. To avoid power saturation, low burning intensities between 10 and 200 μW/cm^2 were selected. In addition, for the hole detection the intensity was reduced by two orders of magnitude. To compare different samples, the burning wavelength was chosen to have the initial optical density in all cases at about 0.7. The normalized hole spectra at

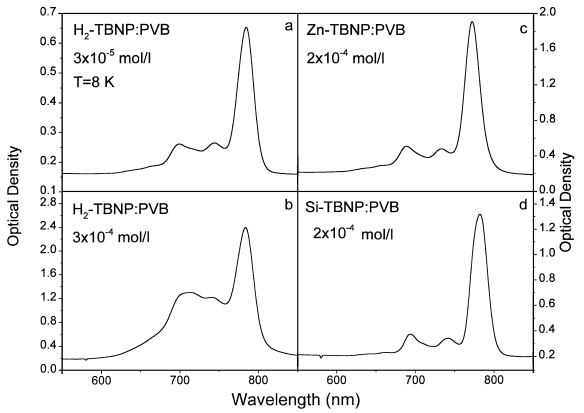

Fig. 1. (a–d) Absorption spectra of several naphthalocyanines at 8 K.

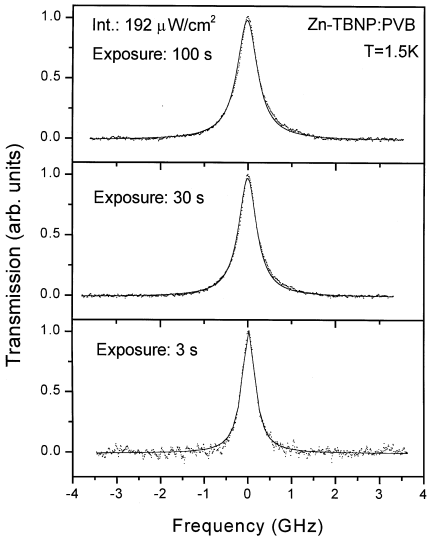

Fig. 2. Normalized spectral hole profiles for Zn-TBNP at 1.5 K at different exposures with burning intensity of 192 μW/cm².

different exposures for Zn-TBNP/PVB are shown in Fig. 2. The hole broadening due to the exposure saturation is clearly seen. The minimal holewidth (see Table 1) was found by extrapolation of the holewidth dependency on burning intensity and on burning time to the zero-intensity zero-exposure limit.

The measured kinetics were analyzed according to the approach presented in Ref. [2] in order to determine the quantum efficiency of PSHB. The following is a brief review of the method for determination of this important parameter.

We express the quantum efficiency, i.e., ratio of molecules participating in hole burning to the total number of photoexcited molecules, in the parameterized form of $\varphi = \exp(-a)$. Following the reasoning in Refs. [3–5], we assume that the parameter a is subject to a Gaussian distribution. Taking into account the dispersion for hole-burning kinetics due to the difference in absorption at the laser frequency for centers within the inhomogeneous band, the random orientation of the absorbing centers with respect to the polarization of the burning light, and the distribution of quantum efficiency, the time dependence $H(t)$ of the sample absorption at the peak of the hole can be calculated as

$$H(t) = B + \frac{3}{2}\frac{D}{w}\sqrt{\frac{4\ln(2)}{\pi}} \times \int_0^{\infty}\int_0^{\pi} \exp\left(-\frac{I\exp(-a)\alpha\sigma\cos^2\theta}{2}t\right) \times I_0\left(-\frac{I\exp(-a)\alpha\sigma\cos^2\theta}{2}t\right)\cos^2\theta\sin\theta \times \mathrm{d}\theta\exp\left(-4\ln(2)\frac{(a-a_c)^2}{w^2}\right)\mathrm{d}a, \quad (1)$$

where a_c and w are, respectively, the center and width of the distribution of the parameter a, $I_0(x)$ is a modified Bessel function of zero-order (calculation $H(t)$ through $I_0(x)$ was used in Ref. [6]), I is the photon flux of the burning irradiation, σ is the

Table 1
Spectroscopic and hole-burning parameters for naphthalocyanines-doped polymers at 1.5 K

Sample	Concentration (mole/l)	Holewidth (MHz)	Inhomog. linewidth (MHz)	σ_h, (cm²)	Efficiency of PSHB $\langle\varphi\rangle$	Distribution parameters		
						Center	Width	B
H_2-TBNP/PVB	3×10^{-5}	150	1.0×10^{7}	8.7×10^{-11}	8.9×10^{-3}	5.88	0	0.42
H_2-TBNP/PVB	7×10^{-4}	100	1.5×10^{7}	6.2×10^{-11}	1.3×10^{-3}	6.92	3.5	0.58
H_2-TBNP/PS	5×10^{-5}	1150	0.9×10^{7}	3.2×10^{-12}	3.2×10^{-2}	3.44	0	0.43
H_2-OBP/PVB	3×10^{-4}	200	1.6×10^{7}	4.5×10^{-12}	1.1×10^{-2}	4.51	0	0.57
Zn-TBNP/PVB	2×10^{-4}	380	1.0×10^{7}	1.7×10^{-11}	1.2×10^{-3}	9.55	6.0	0.28
Zn-TBNP/PS	1.8×10^{-4}	$\approx$ 1000	1.2×10^{7}	$\approx 4.6\times10^{-12}$	$\approx 1.4\times10^{-3}$	9.16	6.7	0.48
Ni-TBNP/PVB	6×10^{-4}	100	1.5×10^{7}	2.1×10^{-11}	6.7×10^{-3}	5.00	0	0.67
Si-NPDO/PVB	2×10^{-4}	400	2.0×10^{7}	8.7×10^{-11}	8.1×10^{-4}	10.06	4.7	0

peak homogeneous absorption cross section, and α is a Debye–Waller factor. Eq. (1) assumes hole burning through the Lorentzian-shaped zero-phonon lines. D is the maximum relative hole depth ($0 < D < 1$), and $B = 1 - D$ represents the fraction of non-burnable background. The integration of a is only over positive values since the quantum efficiency $\varphi < 1$ for all centers.

Two material parameters, α and σ, required for the fitting procedure, were obtained in the following way. The Debye–Waller factor α was estimated for H_2-TBNP/PVB and Zn-TBNP/PVB to be 0.8 and 0.9, respectively. For simplicity we set $\alpha = 1$ for the other materials. The σ was calculated using the low-temperature absorption cross section σ_{inh}, which was determined from the absorption at 8 K and the concentration data, as $\sigma = (\Gamma_{inh}/\Gamma_h)\sigma_{inh}$. The inhomogeneous broadening Γ_{inh}, was determined from the width of the 0–0 electronic transition in the decomposition fit. We suggest that the homogeneous linewidth Γ_h is half of the determined minimal holewidth since no spectral diffusion was observed in the time range of 10–10^5 s. To avoid error due to the hole burning through the phonon sidebands, we fit the experimental kinetics at the initial stages of the hole growth using Eq. (1) with two free parameters, a_c and w. The parameter D was fixed by the independent measurement of the maximal saturated hole depth at the highest experimentally achievable exposures. Another way to find D was to record the kinetics at two reduced burning intensities. Then, the fitting was performed simultaneously for initial segments of these kinetics with fitting parameters a_c, w and D shared for both datasets. Due to the additional dataset, a single set of parameters a_c, w and D can be found. With the distribution parameters a_c and w obtained, we calculated the average quantum efficiency $\langle\varphi\rangle$ of PSHB.

Fig. 3a shows the representative PSHB kinetics for H_2-TBNP in PVB. The experimental kinetics (curve a.1) is satisfactorily described by Eq. (1) with a single value of quantum efficiency (smooth curve) and does not require the introduction of a distribution of φ. This result is a clear sign of the reaction with a constant (non-distributed) value for the quantum efficiency. Due to the presence of two protons in the center of the H_2-TBNP molecule,

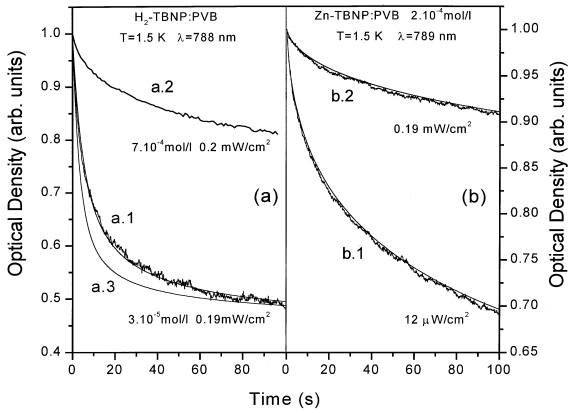

Fig. 3. Hole-burning kinetics for H_2-TBNP (a) and Zn-TBNP (b) at 1.5 K. (a) The experimental kinetics (a.1) was recorded at the intensity 192 $\mu W/cm^2$. The experimental kinetics (a.2) recorded for the sample with concentration 7×10^{-4} mol/l using a laser diode with intensity 0.2 mW/cm^2. All fitting curves used $\alpha = 0.8$ and $\sigma = 2.6 \times 10^{-11}$ cm^2. (b) Kinetics recorded with the intensities 12 $\mu W/cm^2$ (b.1) and 192 $\mu W/cm^2$ (b.2). The corresponding fitting curves were obtained by fitting simultaneously both experimental datasets with the same values of a_c, w, and D, and the proper burning intensity for each dataset. Both fitting curves used $\alpha = 0.9$ and $\sigma = 1.7 \times 10^{-11}$ cm^2.

the most likely hole-burning mechanism is photochemical proton tautomerization, similar to that observed in H_2-phthalocyanine [7]. For illustration purposes, curve a.3 does not fit well the experimental data when the polarization of the laser light is not taken into account. The quantum efficiency and maximal relative hole depth were found from the fitting procedure to be $(8.9 \pm 1.2) \times 10^{-3}$ and 0.58 ± 0.05, respectively. The observed quantum efficiency for H_2-TBNP/PVB is about one order of magnitude higher than that found in H_2-pthalocyanine in polymer matrices [8], and two to three orders of magnitude higher than that found for several nonporphyrin photochemical systems [9].

The experimental hole burning kinetics in Zn-TBNP measured with two substantially different intensities are presented in Fig. 3b (curves b.1 and b.2). Both datasets were fitted simultaneously by Eq. (1) satisfactorily (smooth curves). Parameters a_c, w, and D were found to be 9.15, 6.0 and 0.72, respectively. The value obtained for D is in good agreement with the limit for hole depth of $D = 0.74$

obtained from long 10^5 s kinetics. The average quantum efficiency was calculated to be $(1.1 \pm 0.2) \times 10^{-3}$. The distribution of quantum efficiency is a characteristic feature of the non-photochemical hole-burning mechanism [3]. Consequently, the observed distribution of the quantum yield together with the elimination of the proton tautomerization in metalo-naphthalocyanines suggests that Zn-TBNP possess a nonphotochemical mechanism. This mechanism is likely related to the rotation of the side molecular groups attached to either a relatively rigid phthalocyanine ring or a polymer chain of the host matrix.

A relatively low yield of 7×10^{-6} was estimated for nonphotochemical PSHB in Zn-tetraphenylporphine in PMMA [10]. Our result in Zn-TBNP is two orders of magnitude higher, and only about 10 times less than the yield for photochemical hole burning in H_2-TBNP. The fairly large size of the naphthalocyanine skeleton and the large number of side groups participating in the nonphotochemical PSHB can qualitatively explain this effect. It should be noted that an efficiency as high as 0.11 was reported for nonphotochemical hole burning for Al- phthalocyanine - tetrasulfonate in hyperquenched water [11].

Results for all samples studied are shown in Table 1. Since the detection noise is about 1% for the observed kinetics, the accuracy of the obtained results was mostly determined by the accuracy of the experimental values of σ and was estimated to be $\pm$ 15%. Hole burning in all but one free-base system can be described by a single value of the quantum efficiency. Surprisingly, H_2-TBNP at higher concentration shows a distribution of efficiencies, which is likely related to the overlapping of single molecule and aggregate absorption bands at the laser frequency. Three out of four studied metallo-based systems reveal the broad distribution of hole burning efficiency characteristic of a nonphotochemical hole burning. Only Ni-TBNP/PVB displays a single-valued efficiency of about 0.7%. Thus the mechanism is, likely, photochemical, and should be a subject of future investigation. Another interesting result, is the very low non-burnable background observed for Si-NPDO which makes this system useful for holography applications.

4. Holographic storage

Using the prepared samples of Si-NPDO and H_2-TBNP in PVB and PS, we demonstrated the holographic recording of pages of information at low temperature with good fidelity. The recording set-up is shown in Fig. 4. The light source was a Hitachi 50 mW, Fabry–Perrot temperature controlled laser diode with wavelength centered at 785 nm (@25°C). The wavelength can be coarsely tuned by temperature variation (0. 2nm/°C) and fine tuned by varying the laser diode current at a rate of 2.3 GHz/mA. A computer-controlled current source from ILX Lightwave with 0.1 mA resolution (0.23 GHz) was used to drive the laser diode. An intensity mask consisting of random binary bit patterns of pixel size 100×100 μm is imaged with a 4f system onto the polymer sample placed inside the cryostat. The dimension of the polymer sample is 1×1 cm^2. A 4f imaging system images the mask back onto a STAR cam CCD camera. An iris placed at the Fourier plane of the imaging lens filters the signal from unwanted reflections from the cryostat windows and scattering from the sample.

The reference and signal beams make an angle of 20° outside the sample. The reference consists of a plane wave of 0.2 mW/cm^2 and is equal to the intensity of the signal. At this intensity, we observed a homogeneous line broadening $\sim$1 GHz for the samples mentioned above. A pathlength difference of 14 cm between the reference and signal arm allows a phase shift of $2\pi\Delta\nu(\Delta L/c)$ when the laser is shifted in frequency by $\Delta\nu = 1$ GHz [1]. This phase shift is used to cancel the absorption grating and

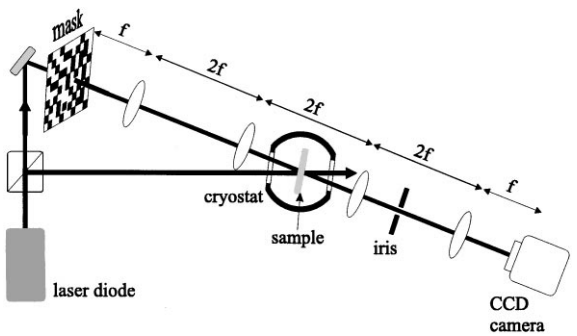

Fig. 4. Experimental holographic setup: image plane recording.

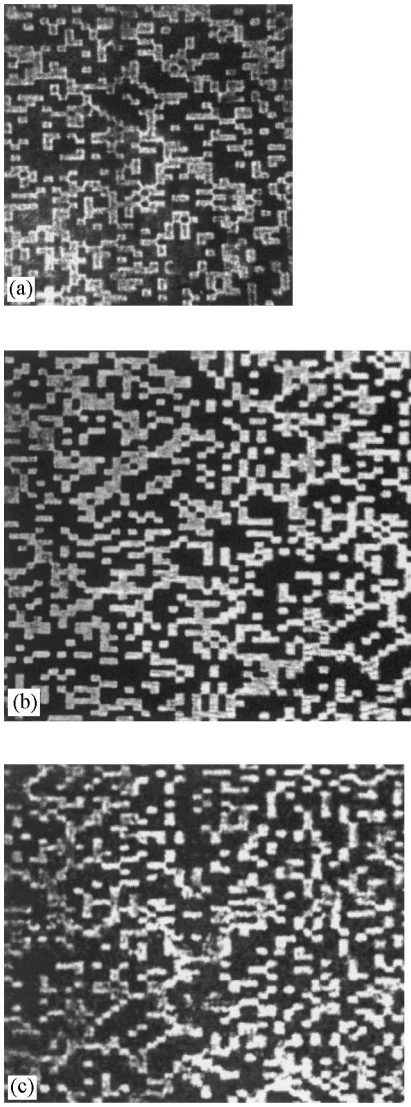

Fig. 5. Reconstruction of the random bit pattern: (a) 400 μm thick H_2-TBN/PVB (788 nm), (b) 400 μm thick Si-NPDO/PVB (787 nm), (c) 1.5 mm thick H_2-TBN/PS (788 nm).

reveals only an index grating in the center of the burning frequency through the Kramers–Kronig relations [12,13]. Holograms were recorded for 4 s. The reconstruction of holograms in 400 μm thick H_2-TBNP/PVB at 788 nm, 400 μm thick Si-NPDO/PVB at 787 and 1.5 mm thick H_2-TBNP/PS at 788 nm are shown in Figs. 5(a)–(c), respectively. The reconstruction from the thick sample shows defects due to non-uniformity. Better optical quality was obtained for the H_2-TBNP in PVB than in the PS matrix. The sample optical densities were 2.0, 2.3, and 7.2 and the absolute diffraction efficiencies were 5×10^{-5}, 7×10^{-5}, and 1.8×10^{-6}, respectively. The low absolute diffraction efficiency is due to lower hole depth and higher absorption. Especially in the case of H_2-TBNP/PVB, the sample with the large concentration of 7×10^{-4} mol/l showed reduced hole depth, probably due to aggregation. The kinetics obtained with the laser diode for that sample is shown in Fig. 3a (curve a.2). We measured a hole depth of 4% with the exposure energy used in the holographic recording. By calculating the diffraction efficiency using the coupled wave analysis and the measured value of the hole depth, we obtained a diffraction efficiency in agreement with the experimental value. If instead the lower concentration sample from Fig. 3 (a.1) had been used, the diffraction efficiency could be as high as 0.8% (computed for a pure absorption grating with 50% hole depth and optical density 0.7). The reconstruction from the thick sample shows defects due to non-uniformity. Better optical quality was obtained for the H_2-TBNP in PVB than in the PS matrix. This preliminary holographic experiment shows that random bit patterns can be recorded in these materials with good fidelity. The relationship between the intensity line broadening and the hole depth at various hole burning frequencies has to be studied further for these materials in order to address the recording rate and storage capacity.

5. Conclusions

Spectral- and hole-burning properties of several free- based and metallo-naphthalocyanines compounds in two polymer hosts were studied for storage applications with diode lasers. Metallo-naphthalocyanines displayed a nonphotochemical hole-burning mechanism, while free-base molecules exhibited the photochemical proton tautomerization mechanism. The minimal holewidth was found to be between 100 and 1200 MHz at 1.5 K. The inhomogeneous linewidth was found to be approximately 10^7 MHz which makes these compounds suitable for storing multiple holograms at different frequencies, and for terahertz bandwidth

storage and communications applications. The hole-burning kinetics was analyzed, and the quantum efficiencies of hole burning were determined for all materials to be between 0.1% and 1%. High-fidelity holograms (data pages) in the transmission geometry were successfully recorded and reconstructed in the materials studied using single-frequency laser diodes.

Acknowledgements

The work was supported by the US Air Force Office of Scientific Research under contracts F 49620-97-1-0486 and F 49620-99-1-0192.

References

[1] B. Plagemann, F.R. Graf, S.B. Altner, A. Renn, U.P. Wild, Appl. Phys. B 66 (1998) 67.
[2] A.V. Turukhin, A.A. Gorokhovsky, Chem. Phys. Lett. 317 (2000) 109.
[3] R. Jankowiak, L. Shu, M.J. Kinney, G.J. Small, J. Lumin. 36 (1987) 293.
[4] A. Elschner, H. Bassler, Chem. Phys. 123 (1988) 305.
[5] R. Richert, J. Chem. Phys. 86 (1987) 1743.
[6] M. Drobizhev, M. Sapozhnikov, Chem. Phys. Lett. 236 (1995) 438.
[7] A.A. Gorokhovskii, R.K. Kaarli, L.A. Rebane, JETP Lett. 20 (1974) 216.
[8] L. Kador, G. Schulte, D. Haarer, J. Chem. Phys. 90 (1986) 1264.
[9] W.E. Morerner, M. Gehrtz, A.L. Huston, J. Chem. Phys. 88 (1984) 6459.
[10] H. Suzuki, T. Shimada, Jpn. J. Appl. Phys. 31 (1992) 706.
[11] W.-H. Kim, T. Reinot, J.M. Hayes, G.J. Small, J. Phys. Chem. 99 (1995) 7300.
[12] A. Rebane, S. Bernet, A. Renn, U.P. Wild, Opt. Comm. 86 (1991) 7.
[13] S. Bernet, B. Kohler, A. Rebane, A. Renn, U.P. Wild, J. Lumin. 53 (1992) 215.